

Preparation and photocatalytic activity of Mo-doped WO₃ nanowires

Xu Chun Song · E Yang · Gang Liu ·
Yong Zhang · Zhi Sheng Liu · Hai Fang Chen ·
Ying Wang

Received: 12 November 2009 / Accepted: 16 January 2010 / Published online: 3 February 2010
© Springer Science+Business Media B.V. 2010

Abstract Mo-doped WO₃ nanowires were fabricated by a hydrothermal method in the presence of K₂SO₄. The physical properties of prepared nanowires were characterized by X-ray diffraction (XRD), energy-dispersive X-ray analysis (EDS), scanning electron microscopy (SEM), and transmission electron microscopy (TEM). The results show that the obtained products are nanowires with diameters ranging between 10 and 20 nm, and lengths of about 600 nm. Its photoactivity was evaluated through the photodegradation of methylene blue (MB) in aqueous solution. Effects of the molybdenum concentration on the photoactivity of the obtained samples were investigated detailedly. The experimental results indicated that the Mo-doping enhanced the photoactivity of WO₃ nanowires.

Keywords Photocatalytic · Doping · Hydrothermal · WO₃ · Nanowire · Water filtration · Organic pollutant

Introduction

Water is a prime source for all living organism including human beings. A number of industrial effluents, agricultural runoff, and chemical spills are directly released into the water systems. The removal of organic pollutants from water is very important for environmental protection and to fulfill the needs for drinking, irrigation, and industrial use (Qamar et al. 2009b). Many different oxide semiconductors have been used as photocatalysts for water decomposition to oxygen and hydrogen (Yu et al. 2009; Liu et al. 2009; Stengl et al. 2009; Zhang et al. 2004; Bamwenda and Arakawa 2001; Chen 2007). Among them, TiO₂ has been dominantly used because of its high activity, long-term stability, low price, and availability. However, The TiO₂ semiconductor has to mainly use ultraviolet irradiation (Yu et al. 2007) due to its wide band gap. The solar spectrum usually contains about 4% UV light. Therefore, many studies have been tried on the direction of utilizing narrower band gap semiconducting materials that undergo intrinsic photoexcitation, charge separation, and subsequently promote photoreactions using near ultraviolet and visible light, which is eventually beneficial for using solar energy as a source of irradiation.

Tungsten oxide and hydrated tungsten oxide are widely used in electrochromic windows, infrared switching devices, photocatalysis, writing-reading erasing optical devices, and gas sensors (Li et al. 2004; Yu et al. 2008b; Zhao et al. 2006; Lee et al.

X. C. Song (✉) · E Yang · Z. S. Liu ·
H. F. Chen · Y. Wang
Department of Chemistry, Fujian Normal University,
350007 Fuzhou, People's Republic of China
e-mail: songxuchunfj@163.com

G. Liu · Y. Zhang
Fuzhou Area Military Representative Office,
350003 Fuzhou, People's Republic of China

2003). Tungsten oxide has drawn more attentions in the applications of photocatalysts because of its relative narrower band gap (between 2.2 and 2.8 eV) (Xin et al. 2009; Wang et al. 2008; Wang et al. 2002; Gondal et al. 2009; Qamar et al. 2009a; Gondal et al. 2007). Yu et al. have reported fabrication of WO_3 hollow microspheres and their photocatalytic activity for the decolorization of rhodamine B aqueous solution (Yu et al. 2008a). Guo et al. have reported the high photocatalytic capability of self-assembled nanoporous WO_3 (Guo et al. 2007). Yu et al. studied photocatalytic activity of flower-like tungsten trioxide assemblies prepared by a simple hydrothermal treatment of sodium tungstate in aqueous solution of nitric acid (Yu and Qi 2009). Metal-doped semiconducting oxides are potential materials for various photocatalyst and photoelectrochemical conversion applications because of its unique physico-chemical properties. Recently, Peng et al. have reported that Dy-doped WO_3 nanoparticles exhibit much better photoactivity and photostability than that of the bare WO_3 (Liu et al. 2007). It is well-known that nanometer-sized inorganic low-dimensional systems exhibit a wide range of optical and catalytic properties that rely sensitively on both size and morphology. However, the investigation on the photocatalytic activity of Mo-doped WO_3 nanowire has never been reported before. The preparation of 1D nanostructured tungsten oxide in mass quantity has been accomplished by heating a tungsten foil, covered by SiO_2 plate, in an argon atmosphere at 1,600 °C (Zhu et al. 1999) or recently by electrochemically etching a tungsten tip, followed by heating at 700 °C under argon (Gu et al. 2002). The 1D nanostructure synthesis using the inorganic salt instead of the surfactant and water-soluble high molecule has strong points in non-pollution, low-cost, easy-cleanout and recovery. In this work, we describe a facile inorganic route for the synthesis of Mo-doped nanowires in aqueous solution. The photocatalytic activities of the as-prepared samples for the methylene blue (MB) photodegradation were investigated.

Experimental section

Fabrication of Mo-doped WO_3 nanowires

All the chemicals were analytic grade reagents without the further purification. Experimental details

were as follows: $\text{Na}_2\text{WO}_4 \cdot 2\text{H}_2\text{O}$ (1 g) and $(\text{NH}_4)_6\text{Mo}_7\text{O}_{24} \cdot 4\text{H}_2\text{O}$ (the atomic ratios of Mo to W = 0, 0.01, 0.03, 0.07, 0.10) were dissolved in 30-mL deionized water to form a transparent solution. A (3 M) HCl solution was added dropwise into the above solution under continuous stirring until tungstic acid was precipitated thoroughly. Next, the centrifuged precipitate was dissolved in 30 mL deionized water, 40 g K_2SO_4 was added to the system and agitated to form starchiness, and then transferred into Teflon-lined autoclave with a capacity of 50 mL. Hydrothermal treatments were carried out at 180 °C for 12 h. After that, the autoclave was allowed to cool down naturally. The final products were collected and washed with deionized water and ethanol several times and dried in air at 80 °C. The Mo-doped WO_3 nanowires were finally obtained. For convenience of description, changing the atomic ratio of Mo to W, the 0.00, 0.01, 0.03, 0.07, and 0.10 doping of molybdenum ions in WO_3 nanowires were marked as A, B, C, D, and E, respectively.

Characterization

The morphologies were characterized using scanning electron microscopy (SEM, Hitachi S-4700, 25 kV) and transmission electron microscopy (TEM, Tecnai G2 F30 S-Twin, 200 kV). The composition of the product was analyzed by energy-dispersive X-ray detector (EDS, Thermo Noran VANTAG-ESI). The X-ray diffraction (XRD, Thermo ARL SCINTAG X'TRA with CuKa irradiation, $\lambda = 0.154056 \text{ nm}$) was used to analysis the crystallinity.

Photocatalytic experiments

The photoactivity experiments on the prepared samples for the photodegradation of methylene blue (MB) were performed at ambient temperature. An 125 W high pressure mercury lamp (GYZ125) was used as a light source. In a typical process, aqueous suspensions of MB (200 mL, $C_0 = 10 \text{ mg L}^{-1}$) and 50 mg of Mo-doped WO_3 nanowires were placed in a vessel. Prior to irradiation, the suspensions were magnetically stirred in the dark for ca. 30 min to ensure the equilibrium of the working solution. The suspensions were kept under constant air-equilibrated conditions before and during the irradiation. pH of the reaction suspension was not adjusted. Analytical

samples (3 mL) were drawn from the reaction suspension every 10 min, and removal of Mo-doped WO_3 nanowires by centrifugation. The changes of absorptions at 665 nm were applied to identify the concentrations of MB using a 721-type spectrophotometer. The percentage of degradation is reported as C/C_0 . C is the maximum peak of the absorption spectra of MB for each irradiated time interval at wavelength 665 nm. C_0 is the absorption of the starting concentration when adsorption/desorption equilibrium was achieved. To test its photocatalytic lifetime, Mo-doped WO_3 nanowires was recycled and reused five times in the decomposition of MB under the same conditions. After each photocatalytic reaction, the aqueous solution was centrifuged to recycle Mo-doped WO_3 nanowires that were then dried at 80 °C for another test.

Results and discussion

Figure 1 showed the XRD patterns of Mo-doped WO_3 nanowires with different content of molybdenum ions. The main peaks can be indexed undisputedly to hexagonal WO_3 (JCPDS card 35-1001). It is worth mentioning that the more the molybdenum ions doped, the narrower and lower was the diffraction spectrum as shown in Fig. 1b–e, which demonstrated

that with the presence of molybdenum ions, the crystallization of the WO_3 nanowires was inhibited. It is interesting to note that the typical MoO_3 XRD peaks were not observed. There are two reasons responsible for this. One probable reason is that the concentration of Mo-doping is so low that it cannot be detected by XRD. The other is that the structure of Mo^{6+} and W^{6+} ions are very similar and the molybdenum ions maybe insert into the structure of WO_3 .

Morphology and particle sizes of the samples were investigated by SEM and TEM. Figure 2a shows the TEM image of pure WO_3 nanowires prepared via K_2SO_4 -assisted hydrothermal route at 180 °C. It can be seen that pure WO_3 products are nanowires with diameters ranging between 10 and 20 nm, and lengths of about 600 nm. Interestingly, when samples prepared at different Mo-doping concentrations, Mo-doped WO_3 nanowires can be obtained in the whole concentrations range under the investigation (Mo/W: 0.01–0.10). It was found that the Mo-doping concentration had little effect on the crystal shapes of products during this range. For example, TEM image of the Mo-doped WO_3 nanowires (D) are shown in Fig. 2b. As shown in Fig. 2c, the SEM image further demonstrated that the Mo-doped WO_3 nanowires (D) have a uniform wire-like morphology. Diameters and lengths of nanowires were consistent with TEM results (Fig. 2b). Energy-dispersive spectrometry (EDS) analysis was employed to determine the composition of the Mo-doped WO_3 nanowires. For example, the EDS patterns of the Mo-doped WO_3 nanowires (D) are shown in Fig. 2d. The EDS results confirm that the obtained products are composed of the WO_3 doped with molybdenum ions. The three major peaks corresponded to tungsten, oxygen, and molybdenum, respectively.

To understand the detailed structural of the WO_3 nanowires doped with different contents of molybdenum ions, the high resolution TEM (HRTEM) technique was employed. Figure 3a is a typical HRTEM image of pure WO_3 nanowires and shows clear lattice fringes. Figure 3b and c are HRTEM images of the Mo-doped WO_3 nanowires (D) and nanowires (E), respectively. It can be seen that with Mo-doping concentration increasing, the lattice fringes slightly blurred. Therefore, it is reasonable to deduce that the larger the amount of Mo-doping, the poorer the crystallization of the WO_3 nanowires.

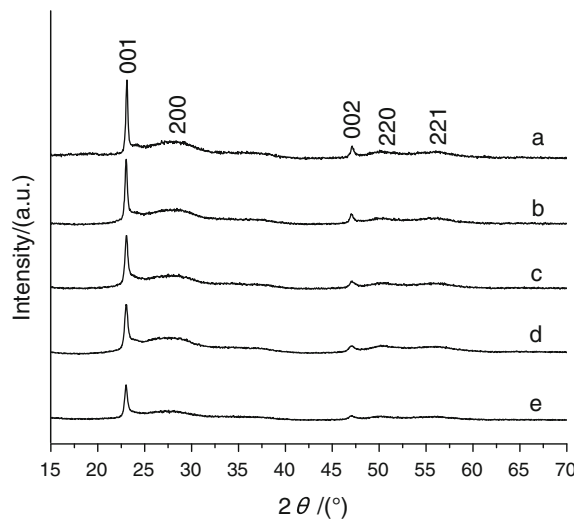


Fig. 1 XRD patterns of the WO_3 nanowires doped with different contents of molybdenum ions. From a–e, the doping ratio of Mo/W was 0, 0.01, 0.03, 0.07, and 0.10, respectively

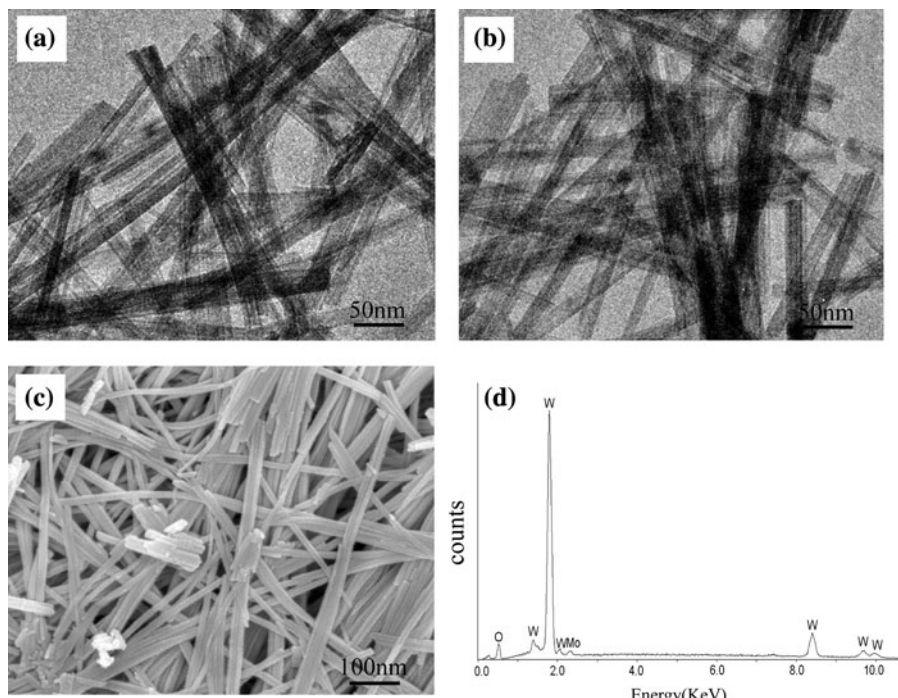


Fig. 2 **a** TEM images of the sample A, **b** TEM, **c** SEM images, and **d** EDS patterns of the sample D

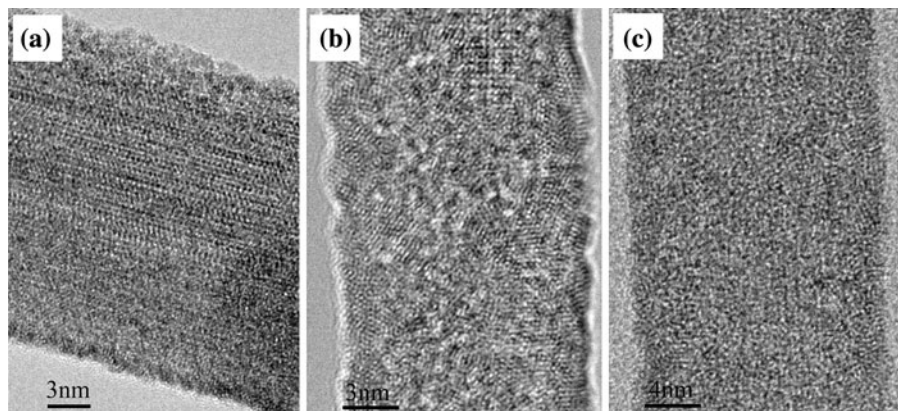


Fig.3 HRTEM images of the WO₃ nanowires doped with different contents of molybdenum ions. From **a–c**, the doping ratio of Mo/W was 0, 0.07, and 0.10, respectively

Figure 4 showed the photocatalytic degradation rates of MB on the Mo-doped WO₃ nanowires with different molybdenum contents. Among the five samples, sample D has much higher photocatalytic degradation rates. For sample D, the MB was removed 94% within 90 min. The blank experiment with catalyst absence was also performed. It can be found that MB is almost not decomposed under the same irradiation time. This result clearly indicates

that molybdenum ions dopant can effectively improve the photocatalytic degradation activities of WO₃ nanowires. When the Mo-doping concentration was lower than 0.07, it is seen from Fig. 4 that as increasing the content of the molybdenum ions, the degradation rate increases. With further increasing Mo-doping concentration, the phototcatalytic activity of WO₃ nanowires decreases obviously. The high phtotcatalytic activity of the sample D is due to the

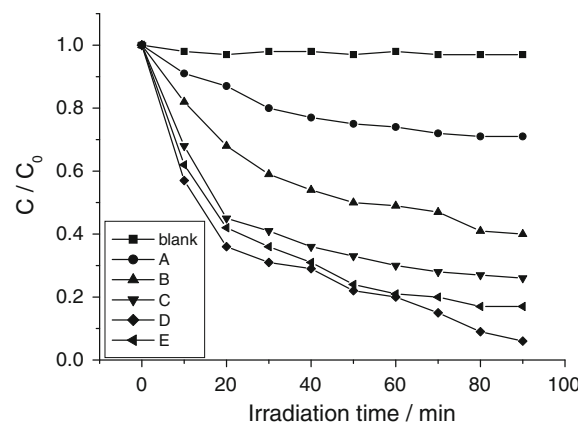


Fig. 4 Photocatalytic degradation of MB by the as-prepared sample

following factor. The molybdenum ions can serve as a mediator of the transfer of interfacial charge at an appropriate doping concentration. The activity evaluation shows that the presence of a small amount of molybdenum ions can enhance the activity, but excessive molybdenum ions are detrimental. This may be due to the fact that a small amount of molybdenum ions can act as a photo-generated hole and a photo-generated electron trap and inhibit the hole-electron recombination.

It is well-known that the preparation condition has relation with crystallization and morphology for the sample. To substantially understand the effect of K_2SO_4 on the Mo-doped WO_3 nanowires, the experiments of the hydrothermal process with different concentration of K_2SO_4 were carried out. The morphologies of the synthesized Mo-doped WO_3 ($Mo/W = 0.07$) with different amounts of K_2SO_4

were shown in Fig. 5a–c. Figure 5a is the SEM image of the sample obtained without K_2SO_4 . The result showed that the products synthesized were only nanoparticles. With the addition of 20 g K_2SO_4 , the morphologies of the synthesized Mo-doped WO_3 shown in Fig. 5b are the nanorods with diameters ranging between 10 and 20 nm, and lengths of about 100 nm. With the addition of 40 g K_2SO_4 , Mo-doped WO_3 nanowires are the major product (Fig. 2c). As the content of K_2SO_4 reaches 50 g, Fig. 5c is SEM image of products and shows similar morphology as observed in Fig. 2c image. Figure 6 shows the effects of the concentration of K_2SO_4 on phase structures of Mo-doped WO_3 nanocrystals. The hexagonal phase of WO_3 (JCPDS card 33-1387) was obtained without K_2SO_4 (Fig. 6a). With the addition of 20 g K_2SO_4 , Fig. 6b exhibited the hexagonal reflections (JCPDS card 35-1001). The XRD results in Fig. 6 also reveal changes in the peak intensities of the obtained Mo-doped WO_3 nanocrystals with different concentration of K_2SO_4 . A distinct sharpening resolution of peaks can be observed in the presence of 40 g K_2SO_4 . The morphologies and dimensions of synthesized nanocrystals were controlled not only by the inner structure, but also affected by the surrounding conditions such as temperature, pressure, and composition of the solution. In our experiments, the presence of K_2SO_4 is important factor influencing the crystallization process and the growth of the Mo-doped WO_3 nanowires. With the addition of different concentration of K_2SO_4 , the corresponding properties of the solution are different in the hydrothermal conditions. The changes in the surrounding conditions would affect the crystal phase, and further affect

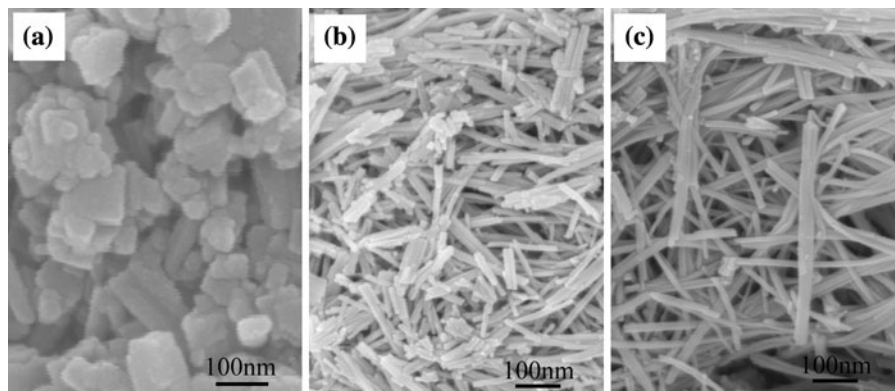


Fig. 5 SEM images of Mo-doped WO_3 synthesized with different amounts of K_2SO_4 : **a** 0 g, **b** 20 g, **c** 50 g

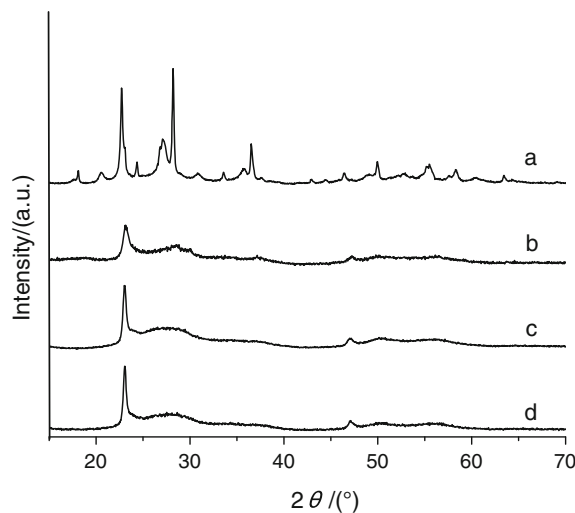


Fig. 6 XRD patterns of Mo-doped WO₃ synthesized with different amounts of K₂SO₄: *a* 0 g, *b* 20 g, *c* 40 g, *d* 50 g

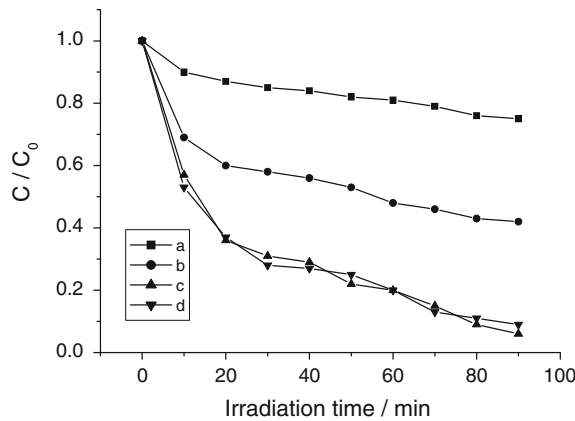


Fig. 7 Photocatalytic efficiency of MB on Mo-doped WO₃ synthesized with different amounts of K₂SO₄: *a* 0 g, *b* 20 g, *c* 40 g, *d* 50 g

the morphologies and crystallization of the WO₃ nanocrystals. Figure 7 shows the effects of K₂SO₄ on the photocatalytic activity of the samples. It can be seen that concentration of K₂SO₄ has a significant effect on the photocatalytic activity of the as-prepared samples. This indicates that the crystal phase and crystallinity are the vital factor that affects the photocatalytic activity of the materials in this work.

The stability of a photocatalyst is important for its application. Herein, the stability of Mo-doped WO₃ nanowires (D) was investigated. After five recycles for the photodegradation of MB, the catalyst did not

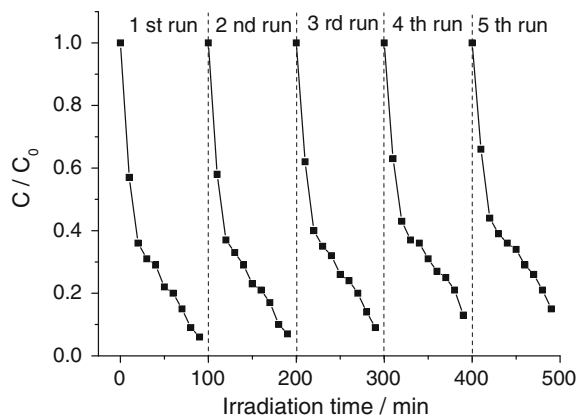


Fig. 8 The lifetime for photodegradation of MB on sample D

exhibit any significant loss of activity, as shown in Fig. 8, confirming Mo-doped WO₃ nanowires (D) is not photocorroded during the photocatalytic oxidation of the pollutant molecules.

Conclusion

A hydrothermal method was developed to the preparation of the Mo-doped WO₃ nanowires. The Mo-doped WO₃ nanowires exhibited the high photocatalytic activity for the decomposition of the aqueous MB. A small amount of Mo-doping could obviously enhance the photocatalytic activity of WO₃ nanowires. At an optimal atomic ratio of Mo to W of 0.07, sample has the highest photocatalytic activity, and after 90 min of irradiation, the MB was removed 94%. The high activities of the Mo-doped WO₃ nanowires could be attributed to the synergistic effects of Mo-doping and crystallinity structure.

Acknowledgment We wish to acknowledge the financial support from the National Natural Science Foundation of China (no. 20873020).

References

- Bamwenda GR, Arakawa H (2001) The visible light induced photocatalytic activity of tungsten trioxide powders. *Appl Catal A* 210:181–191
- Chen CC (2007) Degradation pathways of ethyl violet by photocatalytic reaction with ZnO dispersions. *J Mol Catal A* 264:82–89
- Gondal MA, Sayeed MN, Arfaj A (2007) Activity comparison of Fe₂O₃, NiO, WO₃ and TiO₂ semiconductor catalysts in

- phenol degradation by laser enhanced photo-catalytic process. *Chem Phys Lett* 445:325–330
- Gondal MA, Dastageer A, Khalil A (2009) Synthesis of nano-WO₃ and its catalytic activity for enhanced antimicrobial process for water purification using laser induced photocatalysis. *Catal Comm* 11:214–219
- Gu G, Zheng B, Han WQ, Roth S, Liu J (2002) Tungsten oxide nanowires on tungsten substrates. *Nano Lett* 2:849–851
- Guo Y, Quan X, Lu N, Zhao H, Chen S (2007) High photocatalytic capability of selfassembled nanoporous WO₃ with preferential orientation of (002) planes. *Environ Sci Technol* 41:4422–4427
- Lee K, Seo WS, Park JT (2003) Synthesis and optical properties of colloidal tungsten oxide nanorods. *J Am Ceram Soc* 125:3408–3409
- Li XL, Lou TJ, Sun XM, Li YD (2004) Highly sensitive WO₃ hollow-sphere gas sensors. *Inorg Chem* 43:5442–5449
- Liu H, Peng T, Ke D, Peng Z, Yan C (2007) Preparation and photocatalytic activity of dysprosium doped tungsten trioxide nanoparticles. *Mater Chem Phys* 104:377–383
- Liu Y, Zhang YC, Xu XF (2009) Hydrothermal synthesis and photocatalytic activity of CdO₂ nanocrystals. *J Hazard Mater* 163:1310–1314
- Qamar M, Gondal MA, Hayat K, Yamani ZH, Al-Hooshani K (2009a) Laser-induced removal of a dye C.I. Acid Red 87 using n-type WO₃ semiconductor catalyst. *J Hazard Mater* 170:584–589
- Qamar M, Gondal MA, Yamani ZH (2009b) Synthesis of highly active nanocrystalline WO₃ and its application in laser-induced photocatalytic removal of a dye from water. *Catal Comm* 10:1980–1984
- Stengl V, Bakardjieva S, Murafa N (2009) Preparation and photocatalytic activity of rare earth doped TiO₂ nanoparticles. *Mater Chem Phys* 114:217–226
- Wang HY, Xu P, Wang TM (2002) The preparation and properties study of photocatalytic nanocrystalline/nanoporous WO₃ thin films. *Mater Des* 23:331–336
- Wang S, Shi X, Shao G, Duan X, Yang H, Wang T (2008) Preparation, characterization and photocatalytic activity of multi-walled carbon nanotube-supported tungsten trioxide composites. *J Phys Chem Solids* 69:2396–2400
- Xin G, Guo W, Ma T (2009) Effect of annealing temperature on the photocatalytic activity of WO₃ for O₂ evolution. *Appl Surf Sci* 256:165–169
- Yu J, Qi L (2009) Template-free fabrication of hierarchically flower-like tungsten trioxide assemblies with enhanced visible-light-driven photocatalytic activity. *J Hazard Mater* 169:221–227
- Yu JG, Su YR, Cheng B (2007) Template-free fabrication and enhanced photocatalytic activity of hierarchical macro-mesoporous titania. *Adv Funct Mater* 17:1984–1990
- Yu J, Qi L, Cheng B, Zhao X (2008a) Effect of calcination temperatures on microstructures and photocatalytic activity of tungsten trioxide hollow microspheres. *J Hazard Mater* 160:621–628
- Yu JG, Yu HG, Guo HT, Li M, Mann S (2008b) Spontaneous formation of a tungsten trioxide sphere-in-shell superstructure by chemically induced selftransformation. *Small* 4:87–91
- Yu J, Yu X, Huang B, Zhang X, Dai Y (2009) Hydrothermal synthesis and visible-light photocatalytic activity of novel cage-like ferric oxide hollow spheres. *Cryst Growth Des* 9:1474–1480
- Zhang M, An T, Hu X, Wang C, Sheng G, Fu J (2004) Preparation and photocatalytic properties of a nanometer ZnO-SnO₂ coupled oxide. *Appl Catal A* 260:215–222
- Zhao X, TL Cheung Y, Zhang X, Ng DHL, Yu J (2006) Facile preparation of strontium tungstate and tungsten trioxide hollow spheres. *J Am Ceram Soc* 89:2960–2963
- Zhu YQ, Hu W, Hsu WK, Terrones M, Grobert N, Hare JP, Kroto HW, Walton DRM, Terrones H (1999) Tungsten oxide tree-like structures. *Chem Phys Lett* 309:327–334